RESEARCH REVIEW JOURNALS
Volume-04
Issue-02
February -2019

ISSN: 2455-3085 (Online)
RESEARCH REVIEW International Journal of Multidisciplinary
www.rrjournals.com [UGC Listed Journal]

Optical, Electrical and Thermoelectrical Studies of Bi_2S_3 thin Film, Annealed by dip technique

S.D.Lakade

Bhausaheb Nene College, Pen ,Maharshtra (India)

ARTICLE DETAILS

Article History
Published Online: 20 February 2019

Keywords
Thin film, annealing effect, optical, electrical.

***Corresponding Author**
Email: lakadesd@rediffmail.com

ABSTRACT

In the present paper, we have reported the room temperature growth of bismuth sulphide (Bi_2S_3) thin films by dip method and annealed at different temperature. The films were deposited from a reaction bath containing bismuth nitrate, glycine and sodium thiosulphate. We have analyzed optical, electrical and thermoelectrial properties of Bi_2S_3 thin films. From optical absorption spectra the band gap of the material is estimated to be 1.54 eV at 348 K. 1.49 and 1.44 eV at 423K and 473K. . The value of specific conductance is of the order of $10^{-6}(\Omega\ cm)^{-1}$.Thermoelectric power was found to be 378.45 to 420.27µv/K at 300- 525 K. for sample annealed at 348 K. and 473 K thermoelectric power changes from 390.45 to 435µv/K. The values of series and shunt resistance have been observed to be 211 and 628 Ω annealed at 348 K. and 204 and 618 Ω sample annealed at 473 K.

1. Introduction

Among the V–VI compound semiconductor, Bi_2S_3 has attracted significant interest because of its superior properties such as high absorption co-efficient, direct band gap energy of 1.2–1.7 eV, high figure of merit, and good chemical stability. These intriguing properties make Bi_2S_3 as a techno-logically important material with widespread applications including photovoltaics, photodiode arrays, thermoelectric, switching devices and IR spectroscopy [1–8].Up to now, diverse morphologies of Bi_2S_3 nanostructures including one-dimensional (1D) nanowires, nanoribbons, nanorods ,nano-tubes as well as their complex assemblies such as nano fabrics, necklace architectures, disc-like networks, sheaf-like arrays, snowflake-like patterns and flower-like orurchin-like micro- spheres have been produced [9–19].

Different workers have reported chemical deposition of Bi_2S_3 on different types of substrates with characterization such as chemical deposition [20], interface gas–solution [21], electrode position [22], and spray pyrolysis [23]. Krishnamurthy and Shivkumar [24] deposited

Bi_2S_3films using the hot wall chemical deposition technique. Benramdaneet al. [25] deposited Bi_2S_3 films onto glass substrates byspray pyrolysis method using bismuth chloride and thiourea having bismuth and sulphur source respectively. Pawar et al. [26,27] prepared amorphous Bi_2S_3 and $Sb_{2-x}Bi_xS_3$ films by the solution–gas interface method. Electrode position method was used by Lokhandeand Bhosale [28] to prepare polycrystalline Bi_2S_3 thin films. KrishnaMoorthy [29] has prepared polycrystalline stoichiometric Bi_2S_3films by physical deposition technique. Pramanik and Bhattacharya[30] have also deposited amorphous Bi_2S_3 thin films from an alkalinebath using TEA as a complexing agent. Biswas et al. [31] haveprepared thin films of Bi_2S_3 by solution growth technique using triethanolamine(TEA) as the complexing agent. Lokhande et al. [32,]have deposited thin films of Bi_2S_3 from an alkaline as well as acidicbath using EDTA complexing agent. Ubale et al. [33] have preparedBi_2S_3 thin films by modified chemical bath deposition at room temperature and reported their electrical and optical properties. The non-aqueous chemical deposition of the Bi_2S_3 thin films has been reported by Desai and Lokhande [34] using bismuth nitrate and thiourea in acetic acid and formaldehyde solvents respectively.

We Report synthesis of Bi_2S_3 thin film by dip method. The deposited thin film samples were characterized by various technique such as optical, electrical, thermoelectrial properties are studied.

2. Experimental details

To set up the reaction mixture, 10mL (0.2M) $Bi(NO_3)_3$ became kept in 100mL beaker; different chemical substances have been added in the subsequent series: 4mL (1M) glycine, 15mL (0.2M) sodium thiosulphate. pH of the reaction bath was found to be 4.53. The overall quantity became maintain 50 mL with the help of twice distilled water. The temperature of the reaction mixture becomes manage at 278 K with the help of ice. The reaction mixture became stirred strongly prior to dipping amorphous glass material. The glass plates maintain upright to some extent slanted in a reaction mixture. The hotness of the reaction mixture became subsequently permissible to go up to 298 K extremely gradually. The sample was prepared on each side of substrates. Subsequent to four hours, the substrates have been detached rinsed a number of times with the help of double distilled water. The samples become dried in the atmosphere and conserved in desiccators above anhydrous $CaCl_2$. The achieved sample annealed at 348 K, 423K and 473 K in the atmosphere.

3. Result and discussion

3.1 Optical characterization

The optical absorption spectra of annealed Bi_2S_3 sample have been represented in Diagram 1 (a-c). Annealed samples indicate more transmittance at larger wavelengths and get decreases along with lower wavelength. As the annealing temperature go up, the transmittance gets decreases. Due to annealing, the absorbance diminishes at shorter wavelength. As the annealing temperature of the thin films enhance, absorbance propose an increasing tendency with the wavelength. The absorbance edge shifted towards larger wavelength region. The absorption coefficient of all annealed

samples with analogous wavelength became determined applying relation.

$$\alpha = (A/t) \text{ ----------[1]}$$

Where, A is absorbance and t is thickness. The absorptivity was estimated in the wavelength range 500 to 900 nm. The annealed samples were extremely absorptive. Sample annealed at 348 K offer absorptivity 6 x $10^4 cm^{-1}$ at 500 nm and 1.03 x $10^4 cm^1$ for 900nm. Likewise, sample annealed at 473 K provide absorptivity7.39 x 10^4 cm^{-1} at 500 nm and 1.32 x 10^4 cm^{-1} for 900nm. For lower wavelength the magnitude of absorptivity is high. As the annealing temperature increases absorptivity increases.

The change in optical absorbance with wavelength became considered by using absorption spectrum that indicates the type of electronic transition in between the optical gap. The graph of $(\alpha h\nu)^2$ against hv represented in diagram 2 (a-c). The absorptivity was estimated in the wavelength range 500 to 900 nm. The primary absorption that related to negative charged species traveling as of the valence to conduction band may applied to decide type and magnitude of the band gap energy (E_g). Equation among the absorptivity and the energy of incident beam may represented as[35]

$(\alpha h\nu)^n = A(h\nu - E_g)$-------[2]

In which A is equal to a constant relying at the transition possibility and n is a constant that depends upon the optical transitions. The magnitude of n is hypothetically equivalent to 1/2 or 2, for indirect and direct allowed transition while 1/3 otherwise 2/3 for indirect and direct forbidden transition.[36]The optical gap energy reduced for annealed Bi_2S_3 films with annealing temperature. The band gap was found to be 1.54 eV for sample annealed at 348 K. Similarly, band gap value was found to be 1.49 and 1.44 eV for sample annealed at 423 and 473 K respectively. The decrease in band gap with annealing temperature is probably to increase in grain size, leading to reduction in density of grain boundary trapping centre and improved crystallinity of the film. The graph of $(\alpha h\upsilon)^2$ versus photon energy are straight line in high energy area suggesting direct band to band nature transition. For direct type of transformation the graph of ln(αhυ) against ln (hυ-Eg) must represent a linear nature. Value of slope was found to be close to 2 indicating a single direct type of band gap.

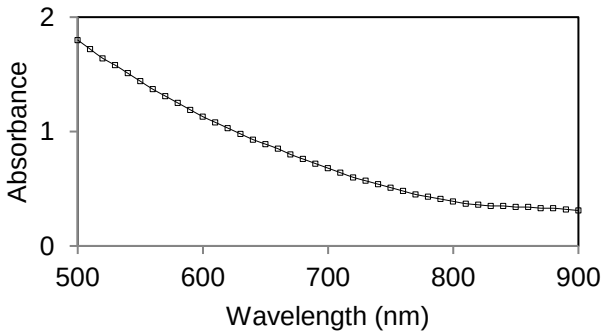

Diagram 1 (a): Plot of absorbance against wavelength for annealed Bi_2S_3 sample at 348 K.

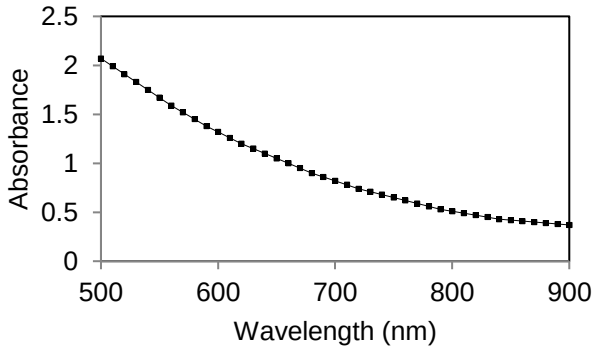

Diagram 1 (b): Plot of absorbance against wavelength for annealed Bi_2S_3 sample at 423 K.

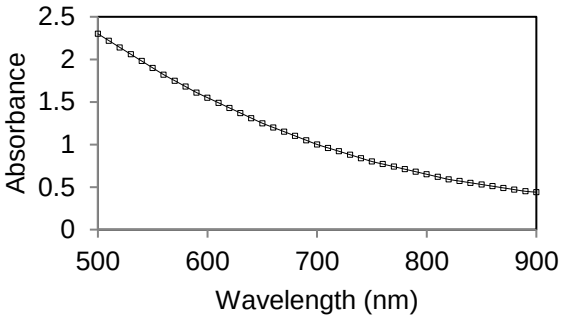

Diagram 1 (c): Plot of absorbance against wavelength for annealed Bi_2S_3 sample at 473 K.

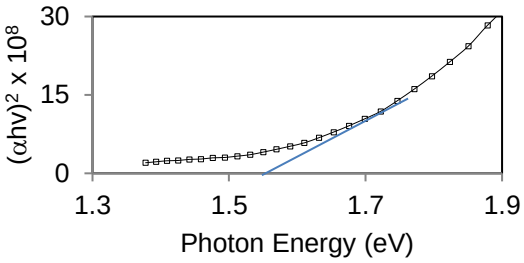

Diagram 2 (a): Graph of $(\alpha h\nu)^2$ with hv for annealed Bi_2S_3 sample at 348 K.

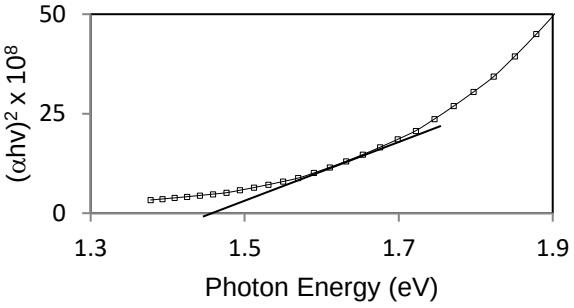

Diagram 2 (b): Graph of $(\alpha h\nu)^2$ with hv for annealed Bi_2S_3 sample at 423 K.

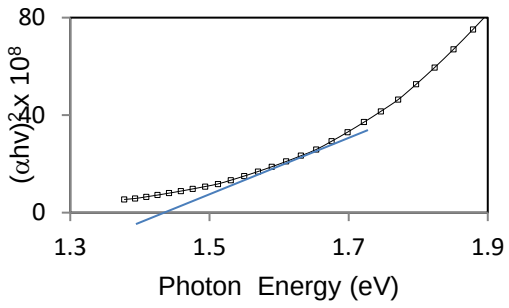

Diagram 2 (c): Graph of $(\alpha hv)^2$ with hv for annealed Bi_2S_3 sample at 473 K.

3.2 Electrical Characterization

The thin film conductivity has been found to depend on different factors like thickness, substrate temperature, deposition rate, and many others. Electrical characteristics are responsive to stoichiometric defect and therefore a wide range of conductance is acquired.[37-39]The conductivity of allthin films became calculated via the use of two probe technique.

The dark electrical conductivity of annealed Bi_2S_3 film at 348K to 473K was determined by using a 'dc' two probe method, in the temperature range 300-525K. The conductance of the thin films will raise with raise in temperature, indicative of semiconducting nature remains of the sample. The value of electrical conductivity for sample 348 K was found to be 1.0 nA at 300K while 0.985 µA at 525K. Similarly, the value of electrical conductivity for sample annealed at 473 K was found to be 1.2 nA at 300K while1.086 µA at 525K. The low value of conductivity for the film may be due to low crystallinity and small thickness of the film.

A common rise in the electrical conductance can be because of reduction in the optical energy of the samples and rise in particle dimension having raise in the annealing temperature. The particle dimension raise as internuclear area decreases and reduce the height of granule junction potential ensuing in increases in the carrier density in addition to the carrier mobility and for that reason electrical conductance. The value of specific conductance was found to be $3.277x10^{-6}(\Omega\ cm)^{-1}$ at 300K and $3.58x10^{-3}(\Omega\ cm)^{-1}$ at 525 K for sample annealed at 348 K. Similarly, specific conductance was found to be $7.526x10^{-6}\ (\Omega\ cm)^{-1}$ at 300 K and $8.619x10^{-3}\ (\Omega\ cm)^{-1}$ at 525 K for sample annealed at 473 K. The specific conductance will increases for annealed films with annealing temperature. The graphs of log conductivity against inverse of temperature are represented in diagram 3 (a-c) for annealed Sb_2S_3 thin samples. It contains two separate areas, confirming the occurrence of two- type conduction method, the small temperature intrinsic and high temperature extrinsic. In the smaller temperature area (300-370 K) is represented via low magnitude of slope. Above this temperature, the curve is characterized by larger slope. The activation energy is estimated usage of expression

$\sigma = \sigma_o \exp(-Ea/KT)$--------[3]

The thermal activation energies determined using the slope of linear portion of log conductivity against inverse of temperature graph. The activation energies for different annealed samples in the range of 348 K to 473 K were found between 0.086 to 0.072 eV for low temperature area. While, for high temperature region activation energies were observed between 0.195 to 0.179 eV. The activation energy found randomly varies with the annealing temperature.

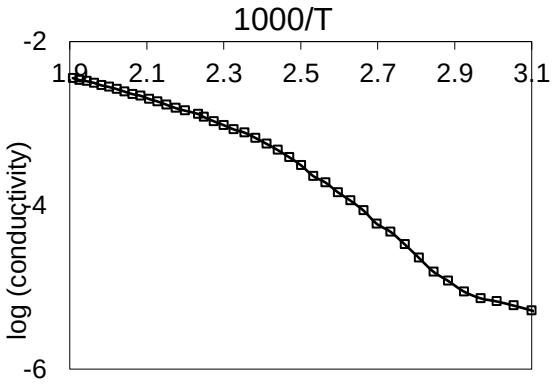

Diagram 3(a): Graph of log conductivity in opposition to inverse temperature for Bi_2S_3 sample annealed at 348K.

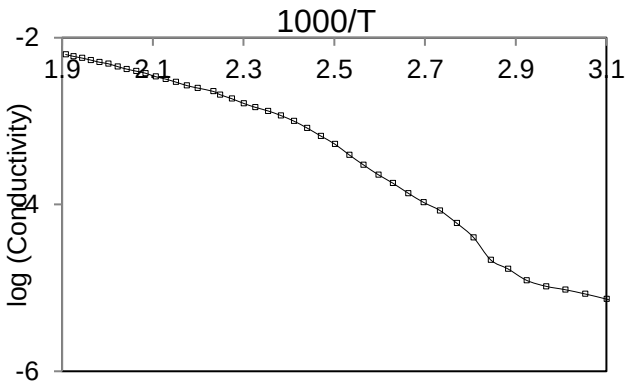

Diagram 3(b): Graph of log conductivity in opposition to inverse temperature for Bi_2S_3 sample annealed at 423K.

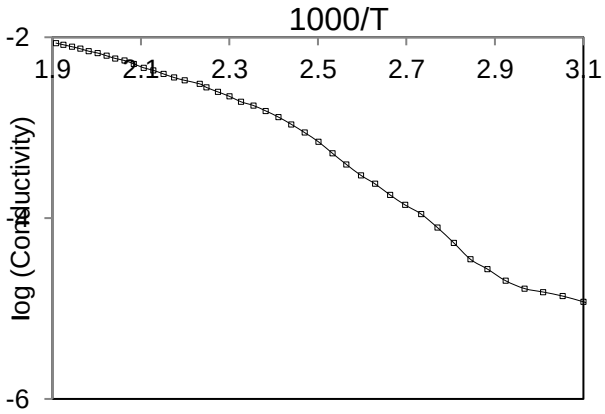

Diagram 3(c): Graph of log conductivity in opposition to inverse temperature for Bi_2S_3 sample annealed at 473K.

3.3 Thermoelectrical Characterization

Thermoelectric power measured for annealed Bi_2S_3 films in the range of 300-525K. This shows rising thermoelectric power with rising temperature for all the films. This indicates degenerate character of the samples. The sign of thermo-electromotive force became positive to hot end w r. t. cold end, that suggests annealed Bi_2S_3 samples shows n-kind

conductivity. The temperature reliance of thermoelectric power was represented in diagram 4 (a-c).

The thermoelectric power is more or less linear in small temperature area, while it varies abruptly at high temperature. As the annealing temperature increases, linearity goes increases. Thermoelectric power was found to be 378.45 to 420.27µv/K in the temperature range from 300- 525 K for sample annealed at 348 K. For sample annealed at 473 K, thermoelectric power changes from 390.45 to 435µv/K as the temperature increase from 300 to 525K. This indicates as the annealing temperature increases the thermoelectric power increases. The linear nature of the graph was observed. The carrier concentration with respect to temperature is calculated using equation.

$\log n = 3/2 \log T - 0.005 P + 15.7198$------[4]

At 300 K, the carrier density became observed to be 4.567×10^{17} and 6.378×10^{17} at 525 K for sample annealed at 348 K. For other extreme i.e. annealing temperature 473 K, the value of carrier concentration was found to be 4.834×10^{17} at 300 K and 6.856×10^{17}at 525 K. As the annealing temperature rise the carrier concentration decreases. Carrier concentration increases as the temperature rise. At low temperature the value of carrier concentration is low, but higher temperature carrier concentration increases. The relation

$\mu = \sigma/ne$----------[5]

was applied to calculate the carrier mobility of all the samples. For sample annealed at 348 K, carrier mobility was found to be 2.468×10^{-5}at 300 K and 2.045×10^{-2} at 525 K. For sample annealed at 473K, carrier mobility was found to be 2.045×10^{-5} at 300 K and 1.003×10^{-2} at 525 K. It was found that carrier mobility rise with raise in temperature. In temperature range 300-400K the change in carrier mobility is very less. But afterwards, it increases steeply.

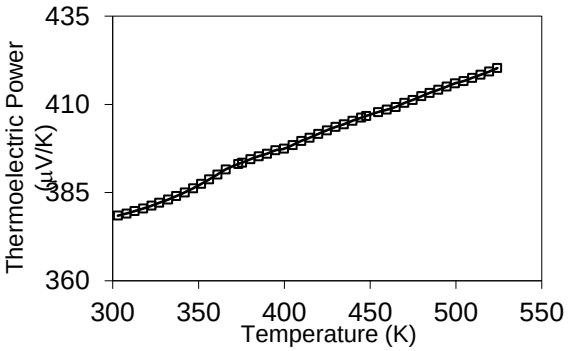

Diagram 4 (a): Thermoelectric power measurement for Bi_2S_3 annealed sample at 348K.

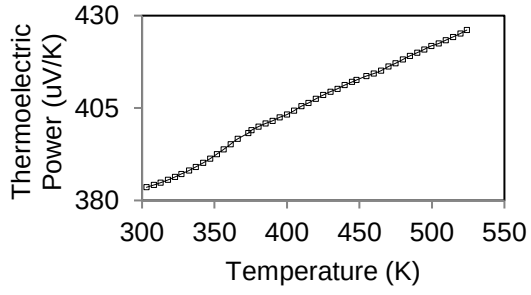

Diagram 4 (b): Thermoelectric power measurement for Bi_2S_3 annealed sample at 423K.

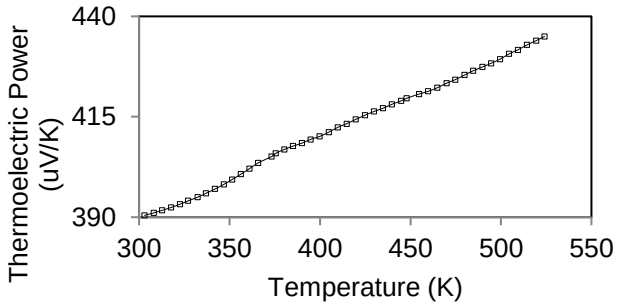

Diagram 4. (c): Thermoelectric power measurement for Bi_2S_3 annealed sample at 473K

3.4 Power Output Characteristics

Photovoltaic production properties for a photoelectrochemical cell (n-annealed Bi_2S_3 | NaOH (1M) + S (1M) + Na_2S (1M) | C (graphite) under the illumination is shown in diagram 5 The open circuit voltage and short-circuit current is obtained to be 232 mV and 1.93 mA/cm^2 correspondingly for photoelectrode annealed at 348 K. The calculations indicate that the fill parameter is 37.67% and solar energy exchange output is 0.103% for sample annealed at 348 K. Similarly, open circuit voltage and short-circuit current is obtained to be 250mV and 2.04 mA/cm^2 correspondingly for photoelectrode annealed at 473 K. Fill parameter was (FF) estimated applying the expression;

$\%FF = [(I_m \times V_m)]/ [(I_{sc} \times V_{oc})] \times 100$ ----------[6]

Wherein I_m is utmost current, V_m is utmost voltage which may be obtained using a power output curve of the cells. The calculations indicate that the fill parameter is 38.42% and solar energy exchange output is 0.113% for sample annealed at 473 K.Series and shunt resistance have been estimated by using the slope of the power production properties applying the expression;

$(dI/dV)_{I=0} = (1/R_s)$ ----------[7]

$(dI/dV)_{V=0} = (1/R_{sh})$ ----------[8]

The values of series and shunt resistance have been observed to be 211 and 628 Ω correspondingly for sample annealed at 348 K. The values of series and shunt resistance have been observed to be 204 and 618 Ω correspondingly for sample annealed at 473 K. Short-circuit current, open circuit voltage, fill parameter and energy output raise as the annealing temperature increases. The series and shunt resistance get reduced as the annealing temperature increases.

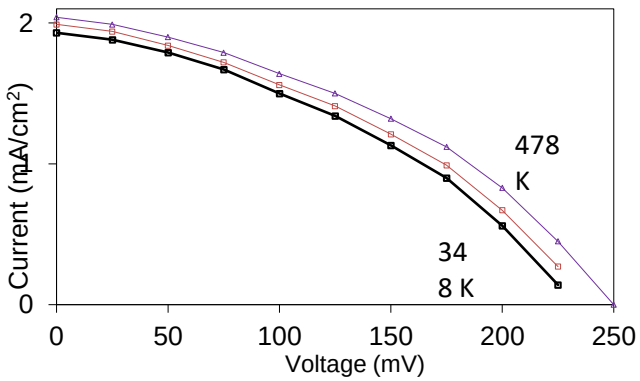

Diagram 5: Photovoltaic output characteristics for annealed Bi_2S_3 photoelectrode using polysulphide electrolyte.

4. Conclusion

1) The optical gap energy reduced for annealed Bi_2S_3 films with annealing temperature. The band gap was found to be 1.54 eV for sample annealed at 348 K. Similarly, band gap value was found to be 1.49 and 1.44 eV for sample annealed at 423 and 473 K respectively. The decrease in band gap with annealing temperature is probably to increase in grain size, leading to reduction in density of grain boundary trapping centre and improved crystallinity of the film.
2) The conductance of the thin films will raise with raise in temperature, indicative of semiconducting nature remains of the sample.
3) It was found that carrier mobility rise with raise in temperature. In temperature range 300-400K the change in carrier mobility is very less. But afterwards, it increases steeply.
4) Short-circuit current, open circuit voltage, fill parameter and energy output raise as the annealing temperature increases. The series and shunt resistance get reduced as the annealing temperature increases.

***Acknowledgement*:**

The author is thankful to Dr.P.A.Chate for encouragement and support. our sincere thank to chemistry faculty. thanks to chemistry laboratory staff for cooperation during research work. I would also like to express my gratitude to Miss. Kajal Subhash lakade for helping me in the research work.

References

1. K. Mageshwari, R. Sathyamoorthy, Mater. Sci. Semicond. Process.16, 43 (2013)
2. B. Pejova, I. Grozdanov, Mater. Chem. Phys. 99, 39 (2006)
3. R. Sathyamoorthy, P. Sudhagar, S. Chandramohan, U. Pal, J.Nanosci. Nanotechnol. 8, 6481(2008)
4. S. Gadakh, C. Bhosale, Mater. Chem. Phys. 64, 5 (2000)
5. R. Mane, B. Sankapal, C. Lokhande, Mater. Chem. Phys. 60, 196(1999)
6. G. Zhu, P. Liu, J. Zhou, X. Bian, X. Wang, J. Li, B. Chen, Mater.Lett. 62, 2335 (2008)
7. C. Tang, Y. Zhang, X. Dou, G. Li, J. Cryst. Growth 312, 692(2010)
8. T. Thongtem, C. Pilapong, J. Kavinchan, A. Phuruangrat, S.Thongtem, J. Alloys Compd. 500, 195 (2010)
9. F. Gao, Q. Lu, S. Komarneni, Chem. Commun. 4, 531 (2005)
10. Z. Liu, S. Peng, Q. Xie, Z. Hu, Y. Yang, S. Zhang, Y. Qian, Adv.Mater. 15, 936 (2003)
11. R. Malakooti, L. Cademartiri, Y. Akc¸akir, S. Petrov, A. Migliori,G. Ozin, Adv. Mater. 18, 2189 (2006)
12. C. Ye, G. Meng, Z. Jiang, Y. Wang, G. Wang, L. Zhang, J. Am.Chem. Soc. 124, 15180 (2002)
13. M. Sigman, B. Korgel, Chem. Mater. 17, 1655 (2005)
14. L. Cademartiri, R. Malakooti, P. O'Brien, A. Migliori, S. Petrov,N. Kherani, G. Ozin, Angew. Chem. Int. 47, 3814 (2008)
15. L. Li, N. Sun, Y. Huang, Y. Qin, N. Zhao, J. Gao, M. Li, H. Zhou,L. Qi, Adv. Funct. Mater. 18, 1194 (2008)
16. J. Tang, A. Alivisatos, Nano Lett. 6, 2701 (2006)
17. Q. Lu, F. Gao, S. Komarneni, J. Am. Chem. Soc. 126, 54 (2004)
18. J. Jiang, S. Yu, W. Yao, H. Ge, G. Zhang, Chem. Mater. 17, 6094(2005)
19. G. Nie, X. Lu, J. Lei, L. Yang, C. Wang, Electro. Acta 154, 24(2015)
20. C.D. Lokhande, A.U. Ubale, P.S. Patil, Thin Solid Films 302 (1997) 1.
21. S.H. Pawar, P.N. Bhosale, M.D. Uplane, S. Tamhankar, Thin Solid Films 110 (1983)165.
22. N.S. Yesugade, C.D. Lokhande, C.H. Bhosale, Thin Solid Films 263 (1995) 145.
23. V.V. Killedar, C.D. Lokhande, C.H. Bhosale, Thin Solid Films 289 (1996) 14.
24. P.A. Krishnamurthy, G.K. Shivkumar, Thin Solid Films 121 (1984) 151.
25. N. Benramdane, M. Latreche, H. Tabet, M. Boukhalfa, Z. Kebbab, A. Bouzidi,Mater. Sci. Eng. B 64 (1999) 84.
26. S.H. Pawar, P.N. Bhosale, Bull. Electrochem. I (1985) 495.
27. S.H. Pawar, P.N. Bhosale, M.D. Uplane, S.P. Tamhankar, Thin Solid Films 110(1983) 165.
28. C.D. Lokhande, C.H. Bhosale, Bull. Electrochem. 6 (1990) 622.
29. P.A. Krishna Moorthy, J. Mater. Sci. Lett. 3 (1984) 551.
30. P. Pramanik, R.N. Bhattacharya, J. Electrochem. Soc. 127 (1980) 2087.
31. S. Biswas, A. Mondal, D. Mukherjee, P. Pramanik, J. Electrochem. Soc. 133 (1)(1986) 48.
32. C.D. Lokhande, V.S. Yermune, S.H. Pawar, J. Electrochem. Soc. 135 (1988)1852.
33. A.U. Ubale, A.S. Daryapurkar, R.B. Mankar, R.R. Raut, V.S. Sangawar, C.H. Bhosale, Mater. Chem. Phys. 110 (2008) 180.
34. J.D. Desai, C.D. Lokhande, Mater. Chem. Phys. 34 (1993) 313.
35. Hankare P., Chate P. (2009) Growth and characterization of WS_2 thin films deposited by dip method. Mater. Chem. Phys. 117: 347-349.
36. Sinaoui A., Trabelsi I., Akkar F., Aousgi F., Kanzari M. (2014) Study of structural morphological and optical properties of Sb_2S_3 thin films deposited by oblique angle deposition. Int. J. Thin Film Sci. Tech. 3: 19-25.
37. Sebastian P., Sivaramakrishan V. (1991) Electrical conduction and transmission electron microscopy studies of $CdSe_{0.8}Te_{0.2}$ thin films. J. Mater. Sci. 26:6443- 6447.
38. Hankare P., Chate P., Delekar S., Asabe M., Mulla I. (2006) Novel chemical synthetic route and characterization of zinc selenide thin films. J. Phys. Chem. Solids 67 (2006) 2310-2315.
39. Theye M. (1984) "Thin Film Technology and Applications", TMH Publishing Co., New Delhi, India.

